

# Analysis of Harmonic Summation in Wind Power Plants Based on Harmonic Phase Modelling and Measurements

Mustafa Eltouki\*, Tonny W. Rasmussen\*, Emerson Guest\*<sup>#</sup>, Lei Shuai<sup>#</sup> and Łukasz Kocewiak<sup>+</sup>

\*Technical University of Denmark – {twr, edagu}@elektro.dtu.dk, <sup>#</sup>Siemens Gamesa Renewable Energy – {emerson.guest, lei.shuai}@siemensgamesa.com, <sup>+</sup>Ørsted Wind Power – lukko@orsted.dk, Denmark

**Abstract**—This article aims to examine the harmonic emission assessment methods based on the IEC 61000-3-6 summation rule in the application of high-power converter-based wind power plants, where only the harmonic amplitude is considered. The IEC 61000-3-6 summation rule could lead to incorrect results due to the assumptions made with respect to the harmonic phase and evaluated from conventional power system harmonics. It has been shown in this paper that this assumption could lead to incorrect harmonic emissions assessment with respect to grid code compliance. Harmonic emission assessment for grid code compliance should be more accurate and the harmonic phase needs to be considered. This paper presents sophisticated phase-aligned measurement results using GPS-disciplined time-base and a proposal of harmonic assessment improvements.

**Keywords**— Background harmonic distortion, Grid code compliance, Harmonic modelling, Harmonic phase modelling Harmonic summation.

## I. INTRODUCTION

Nowadays, the number of wind turbines (WTs) in offshore wind power plants (WPPs) is growing. Furthermore, the complexity of offshore electrical infrastructure is also increasing. This creates challenges in relation to harmonic generation from WT, propagating through resonance circuits and distortion at the point of common coupling (PCC) [1], [2], [3]. Therefore, the assessment of harmonic disturbance from offshore WPPs is becoming an important task.

The estimation of harmonic current and voltage levels at the PCC is typically performed in harmonic studies. This requires detailed and accurate modelling of each WPP component such as cables, transformers, converters. The studies are done to assess the level of harmonic distortion for compliance with harmonic limits imposed by grid operators at PCC, and to assess the harmonic distortion to ensure harmonic compatibility within the WPP electrical infrastructure. Therefore, it is important to assess the harmonic emission as accurately as possible to avoid harmonic underestimation leading to power quality and grid code compliance issues as well as harmonic overestimation leading to unnecessary filtering and capital expenditure.

Typically, the harmonic assessment is performed based on the general summation rule given in IEC 61000-3-6 [4], where assumptions are made about the phase through a summation factor. However, the actual harmonic phase of the individual harmonic is not considered in the standard, which is necessary

for accurate assessment of the harmonic level at the PCC. Particularly, when several WTs are connected in parallel to the PCC, the harmonic phase information indicate whether the resulting harmonic contribution may add or cancel. Harmonic summation considering the harmonic phase is discussed in [5], [6]. Unfortunately, the summation rule used in IEC 61000-3-6 results in underestimation of the harmonic currents emission levels up to the harmonic order 34<sup>th</sup> and overestimation above the harmonic order 35<sup>th</sup> precluding considering the harmonics cancellation opportunities as presented in [7].

Typically, the WPP harmonic performance evaluation is done by measurements procedures as recommended in IEC 61000-21 [8], 61000-4-7 [9] and 61000-4-30 [10]. The harmonic evaluation checks WPP compliance with the grid code and / or IEC 61000-3-6 [4] with respect to the harmonic emission limits. Therefore, it is important that accurate guidelines to estimate the harmonic emission level in WPPs as well as transmission systems are developed. These guidelines and their outcome could have a great impact on the decision making during the design process, by indicating whether filtering is needed or not, in order to improve the design of the WPP.

The state-of-the-art knowledge of harmonic phase of harmonic emission from WTs is quite limited. Therefore, extensive phase-aligned measurements using GPS-disciplined time-base were done at Avedøre Holme offshore wind power plant (AHOWPP) in Denmark. This creates a foundation for investigating harmonic summation considering the harmonic phase information when modelling WPPs. The sampling rate of 44.1 kHz and precise GPS synchronization of the presented one-minute dataset is the first of its kind.

This paper presents the state-of-the-art results and a review of harmonic summation considering Type-4 WTs. The harmonic phase measurement procedure is not well specified in the existing IEC 61400-21 standard [8]. The paper provides additional recommendations on how to measure and process the harmonic phase to fill the gap in the IEC 61400-21 standard [8]. The harmonic emission phase data from the GPS-synchronized measurements is compared with the summation rule given in [4]. Finally, the paper suggests alternative approach for harmonics summation procedures to further improve the IEC summation method.

## II. MEASUREMENT CAMPAIGN AT AVEDØRE HOLME OFFSHORE WIND POWER PLANT

A measurement campaign was performed on AHOWPP and extensive phase-aligned measurements using GPS-disciplined time-base were done, which is the foundation for this study.

### A. System Description

AHOWPP is located in the south of Copenhagen, Denmark, and consists of three identical 3.6 MW Type-4 full-scale converter (FSC) WT's (yielding 10.8 MW) located less than 10 metres from the shore, as shown in Figure 1, which allows access to the offshore WT's by means of a footbridge [1], it has to be noted that AHOWPP is classified as an offshore WPP.



Fig. 1: AHOWPP location in Denmark from [1].

The three WT's each has a Dyn11 step-up transformer 0.69/10 kV for connection to the grid. The WT transformer is connected by means of a circuit breaker to the medium voltage (MV) array cable system (240 mm<sup>2</sup> 10kV aluminium cables). The 10 kV array cable system has a combined length as presented in Table 1.

TABLE 1: AHOWPP ARRAY CABLES DETAILS

WTs	Array cable length [km]	Array cable impedance [ $\Omega$ ]	Array cables capacitance [ $\mu F$ ]
(M1)	2.31	0.361-j0.17	1.23
(M2)	2	0.312-j0.15	1.06
(M3)	1.4	0.218-j0.11	0.74

It should be noted that the array cable system layout is non-uniform leading to differences in the length of the MV cables connected to PCC as presented in Table 1. The installed offshore WT's are fortunately around 300-600 metres from each other, leading to almost the same active power production disregarding the wake effect, thus, no different power bins considering the wake effect are needed in the studies. A simplified diagram of AHOWPP is shown in Figure 2. The specification of the system is shown below:

- 50 kV AC grid voltage
- 0.69 kV WT rated voltage
- 10 kV AC array cable voltage
- Three 3.6 MW WT's

### B. Measurement System Setup

The voltages and currents were measured at several measurement points in AHOWPP as presented in Figure 2. The low voltage (LV) probes were installed at the WT transformer LV-side terminals and the current through the converter inductance were measured using Rogowski coils

installed after the converter reactor according to Figure 2. For brevity the pulse width modulation (PWM) filters and cables have been omitted from Figure 2.

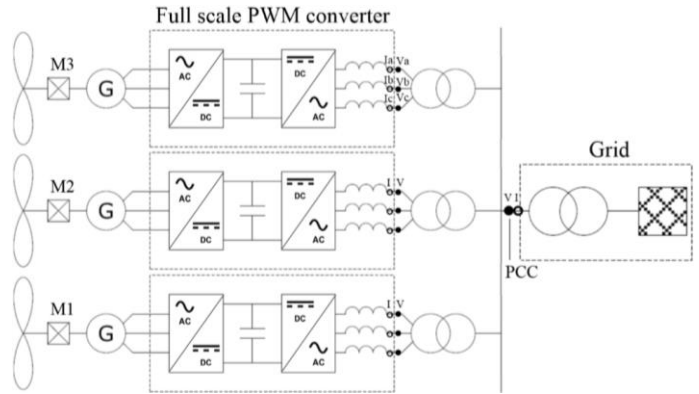


Fig. 2: AHOWPP installed measurement point locations.

All the measurement systems are synchronized by the disciplined clock and digital trigger using GPS-synchronized phase-aligned time-base, which means the number of samples for both the voltages and currents will be exactly the same for all measurement locations in the three WT's and at the PCC [11], [12]. The measurement system software is designed to start according to the digital trigger, which is GPS-synchronized with the other measurement units, specified by the user GPS time-stamp as shown in Figure 3 [12]. The accuracy considerations will be elaborated later in this section.

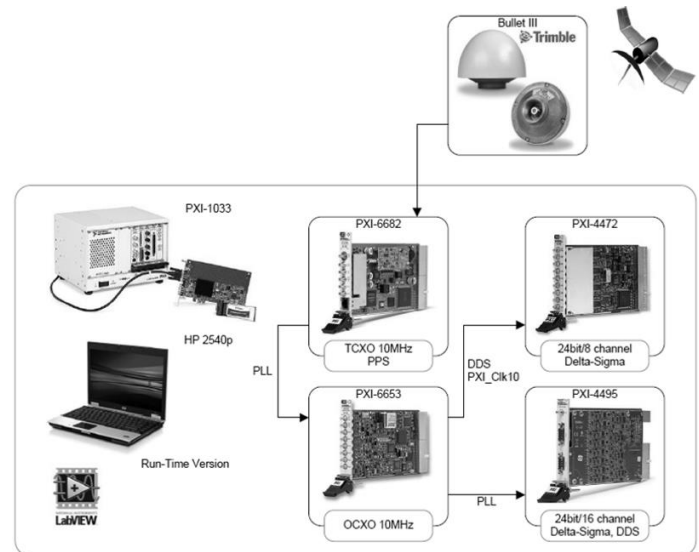


Fig. 3: GPS-synchronized measurement system setup [1].

The two GPS-synchronization methods used are shown in Figure 3.

1) *Synchronization method 1*: The PXI-6682 board receives the GPS timestamp. Next, the GPS board provides a 1 pulse-per-second (PPS) digital rectangular wave which is the basis for synchronizing via the phase-locked loop (PLL) with the PXI-6653 timing board. The timing board is driven by an oven-controlled crystal oscillator (OCXO) to provide the time-base to the PXI-4472 data acquisition (DAQ) board via direct digital

synthesis (DDS) with 1 ppm accuracy. The timing board is needed to provide a stable time-base as the GPS signal is updated with 1 PPS.

2) *Synchronization method 2*: Is very similar to the above, the timestamp is received by PXI-6682 with 1 PPS and locked with PXI-6653 which is further synchronized via PLL with the PXI-4495 DAQ board which is internally providing the time-base. This method is less precise than using DDS, however, still satisfactory for harmonic phase measurements.

In order to minimize the time-base random drift (random walk) the stable OCXO is used to maintain accuracy at 1 ppm for minimum 1 second. If the GPS signal is lost the OCXO will maintain the stable time-base.

All the measurement units used at AHOWPP were synchronized together as presented in Figure 3. A more detailed explanation of the measurement system, measurement software and GPS-synchronization system can be found in [11].

### C. Accuracy and Precision

In order to ensure a proper estimation and evaluation of the harmonic phase and summation, the harmonic magnitude as well as phase need to be measured and aggregated correctly. In particular, the phase requires the fundamental frequency voltage phase as a global reference to evaluate the harmonic phase and possible harmonic summation or cancellation on a system level. In general, the fundamental component of the voltage (or current) can be used as a reference to study the harmonic summation by assessment of the measured phase at multiple locations. The measurement uncertainty requirements for harmonic magnitude is given in IEC 61000-4-7 [9] (Table 1: Accuracy requirements for current, voltage and power measurements). However, the harmonic phase measurement uncertainty assessment is not specified [13]. The main phase measurement uncertainty sources are presented in Figure 4.

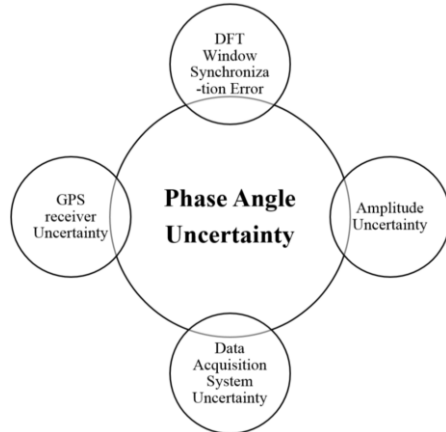


Fig. 4: The phase measurement uncertainty sources [14].

The impact of the harmonic phase measurement uncertainty will be evaluated in the following:

1) *DFT Window Synchronization Error*: The synchronization error due to the discrete Fourier transform (DFT) rectangular window length. According to IEC 61000-4-7 [8] the DFT

window synchronization error is  $\pm 0.03\%$ . This contribution to the phase uncertainty is therefore considered to be insignificant.

2) *Amplitude Uncertainty*: The amplitude uncertainty is mainly depending on the voltage and current measurement equipment accuracy and precision.

3) *Data Acquisition System Uncertainty*: The main DAQ board uncertainties are the temperature drift, offset and system noise. Furthermore, in [12] it was discussed that the anti-aliasing filter delay can also affect the synchronization. The filter delay in this case was compensated, however, 0.25 non-integer sample remain uncompensated [12] and leads to small phase offset.

4) *The GPS Receiver Uncertainty*: The uncertainty represents the delay of timestamp received from the satellites. The accuracy provided by the manufacturer is given in Table 2. Typically, the accuracy of the GPS time signals according to Standard Positioning Service (SPS) used for public applications is guaranteed within  $\pm 170$  ns of UTC for  $1\sigma$  (68 % probability of normal distribution) [1].

TABLE 2: TIMING UNCERTAINTY OF GPS IN ONE-WAY MODE

Service	Uncertainty [ns] 50 <sup>th</sup> percentile	Uncertainty [ns] 1 $\sigma$	Uncertainty [ns] 2 $\sigma$
SPS	$\pm 115$	$\pm 170$	$\pm 340$
PPS	$\pm 58$	$\pm 100$	$\pm 200$

The current measurements were performed using CWT30LF and CWT60LF flexible Rogowski coils with the minimum bandwidth given in Table 3. The parasitic capacitance is compensated due to the long cable (8 m). The integrator to the Rogowski coil is connected via a low-pass filter [12].

TABLE 3: TECHNICAL SPECIFICATION OF THE MEASUREMENT SYSTEM

	DAQ	Input signal	Probe	Bandwidth	Accuracy
M1	4472	Current Voltage	CW30LF, SI-9001	0.055 Hz-6.5 MHz DC-25 MHz	$\pm 1\%$ $\pm 2\%$
M2	4472	Current Voltage	CW30LF, SI-9001	0.055 Hz-6.5 MHz DC-25 MHz	$\pm 1\%$ $\pm 2\%$
M3	4495	Current Voltage	CW60LF, SI-9001	0.055 Hz-3.0 MHz DC-25 MHz	$\pm 1\%$ $\pm 2\%$
PCC	4472	Current Voltage	CW30LF WB3P85, DWB3P8	0.055 Hz-6.5 MHz 1.0 Hz-1.0 MHz	$\pm 1\%$ $\pm 2\%$

Contrary to the current measurement equipment, the voltage measurements were performed with SI-9001 differential voltage sensors with bandwidth of DC-25 MHz as given in Table 3. Capacitive “dead end” T-connectors MV sensors with bandwidth of 1 Hz-1 MHz were installed in all three WTs and at the PCC. The measurement system and measurement equipment have been tested as described in [11] and [12], where the accuracy is shown to be even better than the worst case accuracy stated by the manufacturer. It should be noted that only harmonics with relative high amplitude and within the measurement device tolerances will be considered in the analysis. This will be elaborated in the next section in this paper.

### D. Harmonic Data Processing Algorithm

The data processing algorithm applied for the measured data was based on [4] and [8] and can be summarized as follows:

- 1) Initially, the fundamental frequency component is detected based on Hanning weighted spectrum using an algorithm developed by National Instruments [1]. According to IEC 61000-4-7 [9] a 10-cycle window is recommended for the analysis. In practice, to accommodate possible power system fundamental frequency variation and always assure a 10-cycle window, a longer window is needed, e.g. 10.5 or 11 depending on possible power system frequency variation as specified in the grid code. The frequency detection algorithm can then be applied, and it will provide the actual power system fundamental frequency. Alternatively, other software may use zero-crossing detection algorithms by applying a low pass filter.
- 2) Next, the sampling rate, based on the provided actual power system fundamental frequency component, is adjusted to achieve 10 cycles of 50 Hz. This approach is taken to obtain the integer number of cycles per window and significantly minimize data processing errors, i.e. spectral leakage. The change of sample rate is done using the spline interpolation algorithm [4], which allows to resample the data according to the fundamental frequency selected to equal 50 Hz. This will lead to 8820 samples per 10-cycle rectangular window for the sample rate of 44.1 kS/s.
- 3) The application of DFT to calculate the harmonic components including magnitude and phase for each 10-cycle block of data.
- 4) The definition of harmonic phase global reference to the voltage ( $V_a$ ) fundamental component of the WT 1 (M1), which is arbitrary set to zero. Furthermore, each harmonic phase from DFT is recalculated accordingly to be locked to the global phase reference.
- 5) Calculate the active power production only for the fundamental component according to the IEC standard [8].

### III. RESULTS FROM AVEDØRE HOLME WIND FARM

The measurement procedure given in IEC 61000-21 [8] request zero reactive power injection during the power quality (PQ) assessment of WTs. The measurement campaign was conducted throughout year 2012, where the AHOWPP was operating normally including reactive power injection as well. This is a limitation for AHOWPP that makes the study more complex. However, the obtained measurements can still be considered as sufficient for the validation of the proposed summation rule, which will be elaborately described in the following section.

#### A. Harmonic Measurement Results

The selected aggregation interval of the harmonic spectrum study is one minute. The output active power production from all three WTs during one minute of measurements is calculated according to [9] and can be considered as constant 30% of nominal power. However, Figure 5 shows that the reactive power variation is different for the three WTs. The presented active and reactive power during one minute of measurements

will be used for the analysis of harmonic summation behaviour in the WPP.

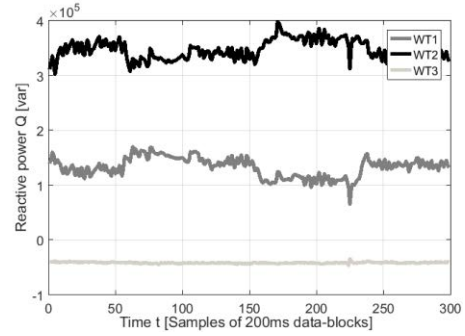


Fig. 5: The reactive power injection for all three WTs during 1 minute of operation, when PWM synchronizations feature is enabled and the active power operating point is approximately 30%.

Moreover, a converter PWM synchronization feature is activated for all three WTs during the measurements [15], which allows the fundamental voltage component to be synchronized with the carrier signal. This allows more accurate estimation of PWM (sideband, carrier group) harmonics as the power system fundamental component phase is linked with the carrier signal in the PWM scheme, i.e. switching frequency is synchronized to the grid frequency. Therefore, it is expected that the displacement angle is fixed  $120^\circ$  for the sideband harmonic from all three corresponding WTs [14].

#### B. Prevailing Angle Ratio

The prevailing angle ratio (PAR) can be employed for aggregation and summation of harmonic phasors. Aggregation (as in IEC 61400-21) in this context means data processing to obtain a combined representation of a number of harmonic components from 10-cycle DFT into one value for a longer period (e.g. 10 second, 1 minute) and summation (as in IEC 61000-3-6) means the total impact of all harmonic sources at a busbar of interest in the power system (e.g. harmonic distortion at the PCC). The harmonic phase information and behaviour can be retained by the aggregation of harmonic phasors based on the prevailing angle. Hence, only the PAR is used to estimate the randomness of the prevailing angle. The PAR can be determined based on:

$$\text{PAR} = \frac{|\sum_{i=1}^n C_{h,i}|}{\sum_{i=1}^n |C_{h,i}|} = \frac{|\sum_{i=1}^n a_{h,i} + jb_{h,i}|}{\sum_{i=1}^n |a_{h,i} + jb_{h,i}|} \quad (1)$$

where  $C_{h,i}$  is the harmonic component complex phasor,  $a_{h,i}$  and  $b_{h,i}$  represent the real and imaginary part of the  $i^{\text{th}}$  window, respectively.

Generally, the PAR result higher than 0.5 indicates a higher degree of deterministic behaviour of the harmonic phase according to [8], whereas the PAR result less than 0.2 indicates a degree of variability resulting in random characteristic of the harmonic phase. This can be used to identify, classify and verify whether the measured data is trustworthy or not.

The current harmonic spectrum plot is presented in Figure 6 (top) and PAR (bottom). It can be clearly seen that the low-order harmonics with relative high magnitude have  $\text{PAR} > 0.6$

as shown by the dotted line in Figure 6 (bottom). On the contrary, the  $PAR < 0.6$  is mainly related to the converter generated high-frequency harmonics due to the PWM scheme.

The observations with respect to the voltage are presented in Figure 7. By comparing Figure 6 and 7 (bottom) it can be seen that the number of harmonics with  $PAR > 0.6$  for higher orders is decreasing due to the measurement accuracy shown in Table 3.

The voltage and current harmonic spectrum plots show that the low values of  $PAR < 0.6$  is related to the very low harmonics magnitude, especially for non-characteristic power system harmonics (e.g. 6<sup>th</sup>, 8<sup>th</sup>) and higher-frequency harmonics disregarding the harmonics emissions up to the 5<sup>th</sup> harmonic order. On the contrary, the lower-frequency harmonics have high values of  $PAR$ , particularly power system characteristic harmonics (e.g. 5<sup>th</sup>, 7<sup>th</sup>).

Moreover, the  $PAR$  can provide some information about the harmonic phase behaviour [14], in order to improve the understanding of the harmonic emission in WPPs. However, it is worth mentioning that non-ideal converter behaviour caused by e.g. dead-time [2], [16], semiconductor voltage drop [17] and background harmonic distortion [18] may influence the harmonic phase and makes the analysis more complicated in relation to the harmonic phase characteristic due to the large variety of technologies (PWM switching pattern, dead-time, control schemes, etc.).

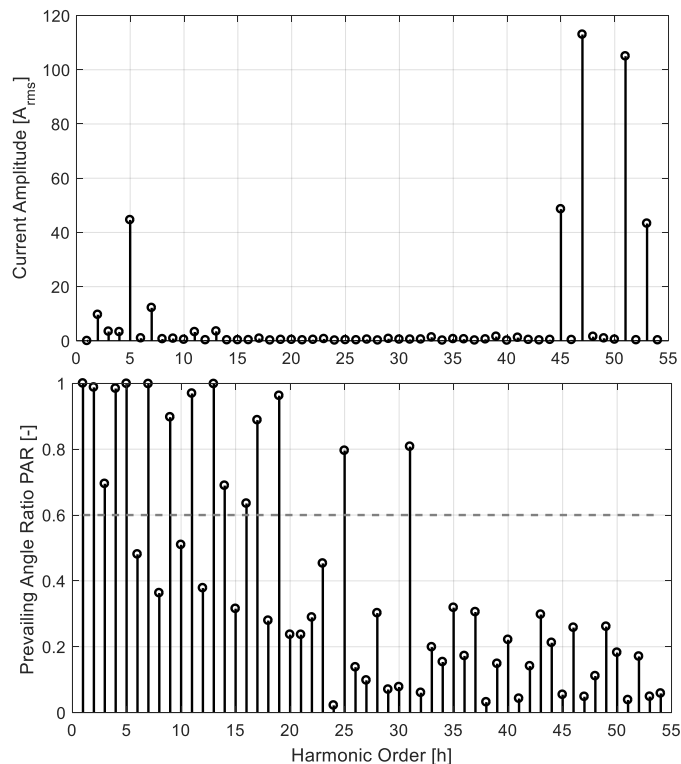


Fig. 6: Current harmonic spectrum for the electrical phase a of WT 1 (M1) (top) and the respective  $PAR$  (bottom) for 1-min period when the carrier signal synchronization feature is enabled

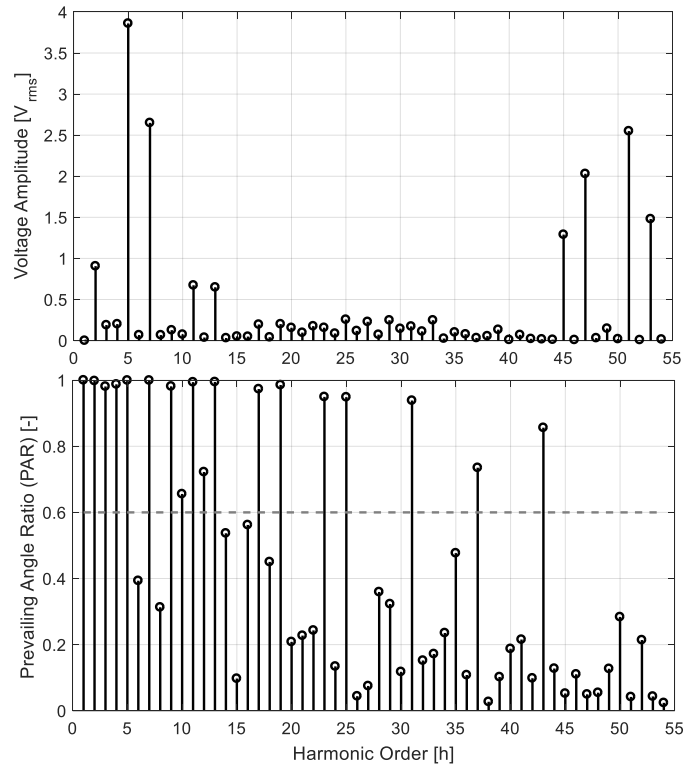


Fig. 7: Voltage harmonic spectrum for the electrical phase a of WT 1 (M1) (top) and  $PAR$  (bottom) for 1-min period when the carrier signal synchronization feature is enabled.

Harmonic emission assessment based on the IEC 61000-3-6 summation rule, where only the harmonic magnitude is known can lead to incorrect results since assumptions are made about the harmonic phase based on choosing a summation factor [7]. It will be shown later in this paper that this assumption cannot be used and can lead to incorrect harmonic emission assessment with respect to the IEC planning / compatibility levels and grid code compliance. The  $PAR$  reflecting the harmonic phase behaviour, which can be used to simplify the harmonics summation approach by simply dividing the harmonics into two groups: (i) those which tend to have a deterministic phase and (ii) those which tend to have stochastic phase characteristic.

#### IV. EVALUATION OF THE SUMMATION RULE AT PCC

The current and voltage spectrum from WT1 (M1) measured at the transformer LV-side is shown in Figure 6 and 7 (top), respectively. Then, from the single WT harmonic spectrum the IEC summation rule is used in order to estimate the harmonic distortion at the PCC. Moreover, the harmonic spectrum from all three WTs including harmonic phase information is used to calculate the harmonic summation at the PCC. Finally, the harmonic distortion estimation based on the IEC summation rule (white), calculated based on measured harmonic magnitude and phase from all three WTs (grey) are compared to the measurements directly at the PCC (black). All harmonic magnitude values are provided at the 95<sup>th</sup> percentile as explained in [4].

From Figure 8 it can be clearly seen that the IEC summation rule underestimates the 5<sup>th</sup>, 7<sup>th</sup>, 11<sup>th</sup>, 13<sup>rd</sup>, 19<sup>th</sup> and 20<sup>th</sup> order harmonic current level at the PCC, which are mainly the power

system characteristic harmonics. Conversely, applying the summation rule leads also to an overestimation of 2<sup>nd</sup>, 3<sup>rd</sup>, 4<sup>th</sup> and higher harmonic order, i.e. 45<sup>th</sup>, 47<sup>th</sup>, 51<sup>st</sup> and 53<sup>rd</sup>. Even a mismatch for higher-frequency harmonics by a factor 4 can be observed for namely 47<sup>th</sup> and 51<sup>st</sup> harmonic order.

Moreover, it should be noted that the estimated harmonic current when including the harmonic phase (grey) does not match the measured harmonic current at the PCC (black). This can be due to the transformer, reactor, WPP and power system modelling uncertainties (e.g. component tolerances, ideal transformer ratio). The WT transformer leakage inductance and copper resistance influence the harmonic current significantly. Furthermore, the uncertainties of measurement system as well as possible harmonic background distortion can lead to discrepancies between measurements and calculations.

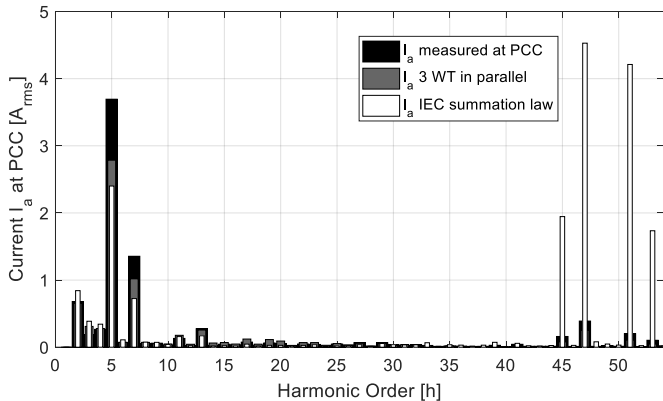


Fig. 8: Comparison of the harmonic current level at the PCC for the phase a.

Furthermore, on one hand the IEC summation rule causes significant overestimation of higher order harmonics (e.g. from PWM) which in reality tend to behave randomly. On the other hand, the harmonics of lower order tend to be underestimated when using the IEC summation rule.

As mentioned earlier, the PAR can be used to reflect the harmonic phase behaviour. The PAR of the harmonic current at the PCC is shown in Figure 9, where it is seen that the harmonics of lower order have a more deterministic phase than harmonics of higher order. Furthermore, the PAR results at the PCC are quite high due to the fact that only one minute of measurement data is considered and the harmonics as well as possible harmonic background distortion trend to vary insignificantly in a short term.

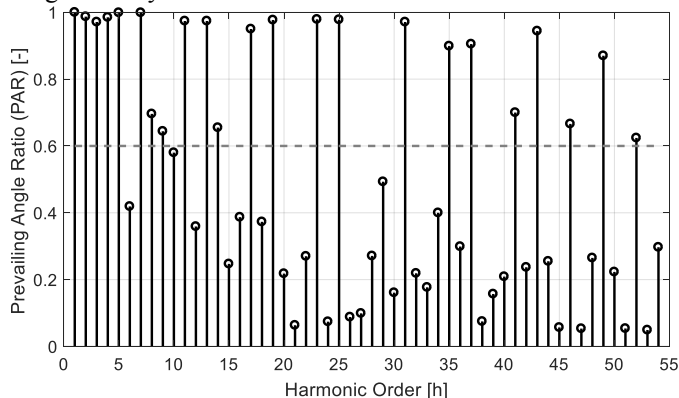


Fig. 9: PAR of the current harmonics at the PCC for phase a.

The same observation as for the current is evident from Figure 10 and 11 also for the harmonic voltage. However, employing the IEC summation rule can sometimes result in amplification of the measurement noise. Moreover, the summation rule causes significant overestimation of higher order harmonics which may be caused by the non-consideration of harmonics cancellation (e.g. from PWM).

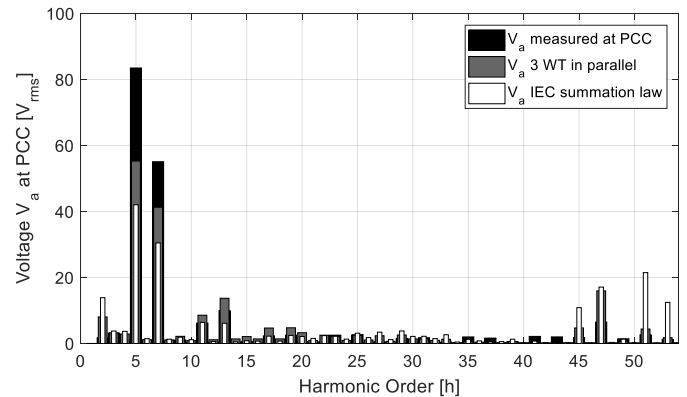


Fig. 10: Comparison of the voltage harmonic level at the PCC for phase a.

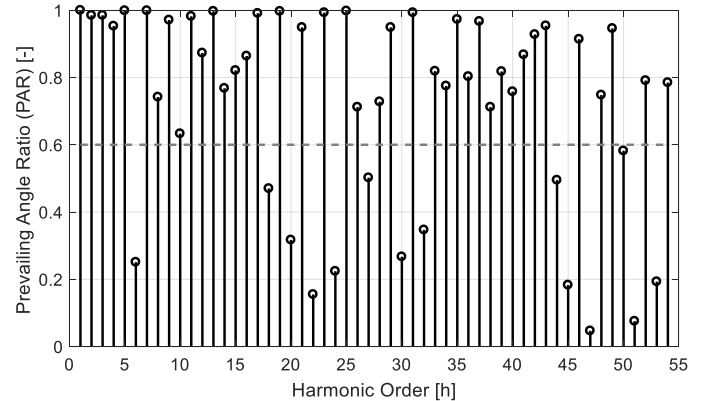


Fig. 11: PAR of the voltage harmonics at the PCC for phase a.

Furthermore, the PAR results of the voltage in Figure 11 indicate a highly degree of deterministic behaviour due one-minute time limitation for this study case. In general, it is rather expected to observe a more stochastic behaviour at the PCC due to the harmonics as well as possible harmonic background distortion trend to vary significantly in a long term.

## V. DISCUSSION

The results from this study show that current harmonic estimated based on both the IEC summation rule and actual phase does not match the measurements at the PCC. This shows that the measurements need to be performed with well-established system conditions which can be reflected in detailed simulations. Furthermore, no-load measurements of the grid and measurement without the PWM filter are recommended to understand the impact of the grid and the harmonic contribution from the WT converter.

Moreover, a sensitivity analysis of the transformer tolerance can be performed to verify the impact of the component uncertainties to conclude the impact and the need of modelling. The performed analysis in this paper has some other limitations which must be mentioned such as the limited aggregation time for PAR results need to be extended with more than one minute

of data. To sum up, the following limitations were observed which can be covered in future studies:

Harmonics with deterministic or stochastic phase characteristics can for some situations be calculated as presented in [16] and [2], however, the phase behaviour can change depending on the WT control, modulation scheme, etc.

Furthermore, more measurement data need to be analysed to provide general conclusions applicable to large WPPs including active and reactive power variation.

The study can be useful to represent similar WTs with the same control and modulation scheme. However, changes in the control algorithm, dead time scheme, modulation technique, etc. can lead to different conclusions and the WT harmonic performance is significantly affected by the factors mentioned above.

## VI. CONCLUSIONS

The analysis of harmonic summation in WPPs based on detailed phase modelling and measurements was presented in this paper. The harmonic phase behaviour for a single WT and at the WPP level, i.e. at the PCC, was presented and the limitations were discussed.

The 95<sup>th</sup> percentile of the aggregated harmonic currents and voltages based on the measurement results including the phase were compared to the corresponding results obtained by the IEC summation rule. The presented results confirm that the assumptions made in the IEC summation rule about the harmonic phase by choosing a summation factor, results in an inaccurate harmonic estimation. Particularly, higher-frequency harmonics tend to be overestimated by applying the summation rule, which is probably caused by non-consideration of harmonic cancellation. Moreover, the measurement noise should be considered before using the summation rule.

The analysis presented in this paper brings better understanding regarding offshore WPP harmonic phase behaviour. The PAR was applied and gave an indication of whether the harmonic phase tends to behave deterministic or stochastic. It was shown that the PAR of the current harmonics provides information and guidelines to the harmonics summation procedure from the IEC 61000-3-6. It was observed that the harmonics can be divided into two groups: (i) with deterministic phase and (ii) with stochastic phase.

The results from this study, in general, give an overview of how harmonic behaviour on a system level and it creates a basis for furthermore advanced studies on harmonics propagation of such complex systems as offshore WPPs. The presented analysis creates a basis for more advanced in-depth studies.

## ACKNOWLEDGMENT

This work was supported by the Technical University of Denmark, Ørsted Wind Power and Siemens Gamesa Renewable Energy, DK. The authors would like to express their appreciation to Troels Stybe Sørensen from Ørsted Wind Power for his valuable inputs.

## REFERENCES

- [1] L. H. Kocewiak, "Harmonics in Large Offshore Wind Farms," PhD Thesis, Aalborg Universitet, 2012.
- [2] E. Guest, T. W. Rasmussen and K. H. Jensen, "Probabilistic Harmonic Modeling of Wind Power Plants," in *16th International Workshop on Large-Scale Integration of Wind Power into Power Systems as well as on Transmission Networks for Offshore Wind Power Plants*, Berlin, Germany, 23–27 October 2017.
- [3] C. F. Jensen, Z. Emin and Ł. H. Kocewiak, "Amplification of harmonic background distortion in wind power plants with long high voltage connections," in *CIGRÉ Biennial Session*, Paris, France, 21-26 08 2016.
- [4] IEC 61000-3-6:2008, "Electromagnetic compatibility (EMC) – Part 3-6: Limits – Assessment of emission limits for the connection of distorting installations to MV, HV and EHV power systems".
- [5] K. V. Reusel and S. Bronckers, "Summation Rule for Wind Turbines' Harmonics Challenged by Measurements," in *17th International Conference on Harmonics and Quality of Power*, Belo Horizonte, Brazil, 16-19 October 2016.
- [6] Y. Xiao and X. Yang, "Harmonic Summation and Assessment Based on Probability Distribution," *IEEE Transactions on Power Delivery*, vol. 27, no. 2, pp. 1030-1032, April 2012.
- [7] F. Ackermann, H. Moghadam, S. Rogalla, et al, "Large Scale Investigation of Harmonic Summation in Wind- and PV-Power Plants," in *16th Wind Integration Workshop 2017 : International Workshop on Large-Scale Integration of Wind Power into Power Systems as well as on Transmission Networks for Offshore Wind Power Plants*, Berlin, Germany, 25-27 October 2017.
- [8] IEC-61400-21:2008, "Wind turbines – Part 21: Measurement and assessment of power quality characteristics of grid connected wind turbines".
- [9] IEC-61000-4-7:2002, "Electromagnetic Compatibility (EMC) – Part 4-7: Testing and Measurement Techniques – General Guide on Harmonics and Interharmonics Measurements and Instrumentation for Power Supply Systems and Equipment Connected Thereto".
- [10] IEC 61000-4-30:2015, "Electromagnetic compatibility (EMC) – Part 4-30: Testing and measurement techniques – Power quality measurement methods".
- [11] Ł. H. Kocewiak, J. Hjerild, T. Sørensen, C. L. Bak, I. Arana and J. Holbøll, "GPS synchronization and EMC of harmonic and transient measurement equipment in offshore wind farms," *Energy Procedia*, vol. 24, pp. 212-228, 2012.
- [12] L. H. Kocewiak and A. Baloi, "Evaluation of Power Quality Monitoring Systems in Offshore Wind Farms," in *13th International Workshop on Large-Scale Integration of Wind Power into Power Systems as well as Transmission Networks for Offshore Wind Farms*, Berlin, Germany, 11-13 November 2014.
- [13] J. Meyer, A. M. Blanco, R. Stiegler and M. Schwenke, "Implementation of harmonic phase angle measurement for power quality instruments," in *IEEE International Workshop on Applied Measurements for Power Systems*, Aachen, Germany, 24 October 2016.
- [14] M. Eltoui, "Analysis and Modelling of Harmonic Emission Aggregation for Offshore Wind Farms, MSc," Department of Electrical Engineering, The Technical University of Denmark, Copenhagen, Denmark, 2018.
- [15] R. Jones, R. Vernon Fulcher and H. Stiesdal, "Control methods for the synchronization and phase shift of the pulse width modulation (PWM) strategy of power converters". Patent US9293921B2, 22 03 2016.
- [16] E. Guest, K. H. Jensen and T. W. Rasmussen, "Sequence Domain Harmonic Modeling of Type-IV Wind Turbines," *IEEE Transactions on Power Electronics*, vol. 33, no. 6, pp. 4934 - 4943, 02 August 2017.
- [17] M. Eltoui and T. W. Rasmussen, "Spectrum analysis of a voltage source converter due to semiconductor voltage drops," in *19th European Conference on Power Electronics and Applications*, Warsaw, Poland, 11-14 Sep. 2017.
- [18] L. S. Christensen, J. G. Nielsen and T. Lund, "Using Prevailing Angle of Harmonics to Distinguish between Background Noise and Emission from a Turbine," in *16th International Workshop on Large-Scale Integration of Wind Power into Power Systems as well as on Transmission Networks for Offshore Wind Power Plants*, Berlin, Germany, 23–27 October 2017.